THE JOURNAL OF PHYSICAL CHEMISTRY Letters

Letter

pubs.acs.org/JPCL

DPD Simulation of Protein Conformations: From α-Helices to β-Structures

Aleksey Vishnyakov,[†] David S. Talaga,[‡] and Alexander V. Neimark*[,†]

[†]Chemical and Biochemical Engineering, Rutgers University, New Jersey

[‡]Chemistry and Biochemistry, Montclair State University, New Jersey

Supporting Information

ABSTRACT: We suggest a coarse-grained model for DPD simulations of polypeptides in solutions. The model mimics hydrogen bonding that stabilizes α-helical and β-structures using dissociable Morse bonds between quasiparticles representing the peptide groups amenable to hydrogen bonding. We demonstrate the capabilities of the model by simulating transitions between coil-like, globular, α-helical, and β-hairpin configurations of model peptides, varying Morse potential parameters, the hydrophobicities of residue side chains, and pH, which determines the charges of residue side chains. We construct a model triblock polypeptide mimicking the sequence of residues α-synuclein at two different pHs. The conformations of this model polypeptide depend on pH similarly to the behavior observed experimentally. The suggested approach to accounting for hydrogen bond formation within the general DPD framework may make the DPD method a competitive alternative to CGMD for modeling equilibrium and dynamic properties of proteins and polypeptides, especially during their transport in confined environments.

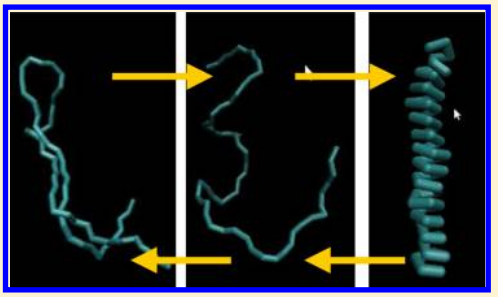

SECTION: Biophysical Chemistry and Biomolecules

Tremendous progress has been made in molecular simulations of biopolymers (e.g., refs 1−12), yet the wide range of length scales and time scales relevant to living systems continues to pose significant challenges to such simulations. The crowded and confined environment of cells requires that biopolymers undergo large conformational transformations during function and transport. The fundamental challenge is to account for a complex interplay of properties across many characteristic length and time scales (1 nm−1 μm, 1 ns−10 ms) while obtaining reliable statistics for these stochastic processes. Relevant macromolecular properties include monomer size, persistence length, gyration radius, length of secondary structures, chain length, and the nature of environmental conditions including confinement. Among the most challenging biomolecules are polypeptides and proteins, for their size and structural diversity. When conditions and/or the sequence result in significant disorder in the polypeptide, structures can fluctuate between folded, unfolded, globular, coil-like, α-helical, β-hairpin, and others in varying combinations depending on the hydrophilic/hydrophobic, electrostatic, and other interactions involving backbone and side-chain functional groups. The time scales of these structural changes can be very long compared to the capabilities of traditional molecular dynamics (MD). These challenges can be met by coarse-grained representation of biomolecules.

The most widely used and currently most powerful method for biomolecule simulation at long length and time scales is coarse-grained molecular dynamics (CGMD).[1,3−6,8,10,13,14] CGMD methods with hard-core particles were recently applied to model membrane proteins.[1,6] The main problem in the current approaches to coarse-grained modeling of proteins and polypeptides in solutions is a lack of established methods to simulate hydrogen bonding between the skeletal peptide groups, which play one of the main roles in secondary structure formation[15] and whose effect is often mimicked by forces of very different nature. Simplified or minimalistic models of proteins within the framework of CGMD have been suggested to treat long time scale phenomena. Nguyen and Hall[8] used discontinuous MD simulation and an intermediate-resolution model (PRIME) to mimic amyloid fibril formation by polyalanine peptides. Marchut and Hall[4,5] extended PRIME to treat aggregation of polyglutamine (pGLN), a disordered protein prone to fibrillar aggregation. A minimalistic MD model of pGLN was also suggested by Digambaranath et al.[16] Wang and Voth[10] used a multiscale coarse-graining method to construct solvent-free coarse-grained models for pGLN peptides having various repeat lengths.

CGMD modeling of folded proteins in solutions often involves geometry enforcement using nondissociable bonds. For example, in their DPD modeling of membrane proteins, de Meyer et al. and Morozova et al.[7,17] represented proteins as soft bodies composed of hydrophilic and hydrophobic beads connected by bonds in a special way to achieve the desired specific arrangement of hydrophilic and hydrophobic segments.

Received: August 27, 2012
Accepted: October 3, 2012
Published: October 3, 2012

Similarly, the torsion potential can be used to enforce an α-helical structure of the protein.[6,18] Enforcing a desired secondary structure is appropriate for static structures with small excursions from known folded geometries. Such an approach breaks down for phenomena involving protein transport and restructuring such as unfolding during protein translocation through nanopores[19] or disordered ensembles of structures. It is desirable to enable modeling of secondary structure formation and destruction under variable environmental conditions that is compatible with efficient modeling of protein transport. Such large-scale structural changes suggest the need for replacing harmonic bonds with dissociating bonds.

Existing CGMD studies focus primarily on static and short time properties of the biomolecules reproducing atomic-level structure and thermodynamic variables while modeling small-scale fluctuations from a known geometry. Modeling cellular and other long time scale phenomena requires a proper treatment of transport properties, adding the requirement that hydrodynamic behavior and the effects of dissipation and thermal fluctuations be accurately included. By its nature, CGMD has difficulty reproducing hydrodynamic behavior as the coarse-graining removes the degrees of freedom that are responsible for dissipation.

By contrast, dissipative particle dynamics (DPD) explicitly accounts for drag and random forces between soft and permeable coarse-grained particles and explicit solvent.[20] DPD can provide an accurate bridge from the atomic scale to the hydrodynamic scale, which is vital for reproducing transport of biopolymers in crowded and/or confined environments. DPD has been actively employed in modeling polymers and various self-assembled systems including lipid membranes,[12,21,22] but application of explicit solvent DPD to peptides has thus far been limited to simplistic models of membrane proteins.[23,24] Implicit solvent Brownian dynamics (BD) simulations of helical peptide dynamics have also been attempted.[18] For soft particle approaches as DPD and BD, accounting for charge distribution also poses a problem, and direct inclusion of electrostatic forces in DPD simulations of biosystems is rare.[9] The distribution of charges is particularly relevant for modeling movement of nanoconfined polypeptides in the presence of strong electric fields.[19]

In this Letter, we introduce a novel approach to efficient modeling of polypeptide and protein secondary structures and their transitions by means of DPD that lays the groundwork for future development of comprehensive computational tools for studies of cellular and biotechnological phenomena across new length and time scales. The novelty of the proposed model is the approach employed to account for the effect of formation and dissociation of H-bonds in DPD simulations, thus enabling better modeling of secondary structural changes while preserving proper hydrodynamics. We demonstrate the feasibility of the approach, first by modeling the formation and stability of α-helices and β-hairpins in different model chain proteins by varying the degree of hydrophobicity and charge distribution. Second, we consider a model polypeptide composed of hydrophilic and hydrophobic blocks that mimic the main structural features of α-synuclein (αSyn), a protein with an intrinsically disordered monomeric state that has been implicated in Parkinson's disease (PD).[25]

For DPD simulations, the peptide was modeled as a sequence of soft quasiparticles ("beads"), connected by harmonic and Morse bonds; water solvent was composed of single beads. One amino acid residue is represented by a skeleton bead plus one or two side-chain beads, where needed. This scheme is natural and was previously employed in coarse-grained simulations of peptides.[10] The skeleton bead effectively represents one glycine residue in the peptide chain. The effective volume of glycine in proteins is 60 Å,[3,26] which conveniently equals twice the effective volume of a water molecule as calculated from the liquid density. Accordingly, the bead size was set to R_c = 5.64 Å. Water "W' beads each represent two water molecules. Interpolation of the experimental water compressibility onto the correlation between simulated compressibility of our coarse-grained model yielded $a_{WW} = 50\ kT/R_c^2$; see Figure S1 in the Supporting Information. This parameter was applied to repulsive interactions between the beads of the same type, a_{ii}. S beads are mildly hydrophobic, which is accounted for by setting the mismatch parameter to $a_{SW} = 55kT/R_c^2$. The residue side chains are modeled with hydrophobic (T) and hydrophilic (H) beads with the mismatch parameters $a_{TW} = 63kT/R_c^2$, $a_{HW} = 50kT/R_c^2$, and $a_{HS} = a_{TS} = a_{HT} = 58kT/R_c^2$. A general description of the DPD method and simulation details are given in the Supported Information.

The secondary structure of proteins is largely determined by >N−H···O═C< hydrogen bonds between the skeletal groups as well as by the chain stiffness due to the limited torsion angles. A coarse-grained model is unable to treat the formation and breakup of the individual H-bonds; however, it can mimic their effect by allowing skeletal particles to form dissociable bonds. The dissociable bond is described by a Morse potential,[27] which is has been applied in atomistic MD simulations, for example, in aqueous solution modeling.[28,29] The Morse potential $E_M(r) = K_M[1 - \exp(\alpha\ (r - r_e)^2]$ at $r < r_M$ has four parameters that control the behavior of the effective H-bond; these are the energy well deepness K_M and width α, equilibrium distance r_e, and a cutoff distance r_M, $E_M(r) = 0$ at $r > r_M$ to improve computational performance for broken H-bonds. As we show below, the Morse potential can be tuned to mimic the effects of hydrogen bonding in proteins because it allows bond formation/dissociation and has a limited range. Its function is similar to that of the square-well potential used in the PRIME CGMD model to represent hydrogen bonding.[30] We assert that a dissociable potential provides significant advantages over the methods previously attempted in the literature. The H-bonds to the solvent are not taken into account explicitly in the proposed model, but the Morse potential is interpreted as representing the net effect of exchanging a backbone−solvent for backbone−backbone interaction. The chain stiffness is accounted for by introducing additional potentials between non-neighboring bonds, as described below.

Helical structures in proteins are stabilized by "vertical" >N−H···O═C< hydrogen bonds connecting nonadjacent residues. One helical turn includes approximately four residues (we do not attempt to enforce the helical wheel of 3.6 residues per turn.[31]). To model helical structures, we introduced two sets of Morse bonds, 1−3 Morse bonds between S beads separated by two harmonic bonds and 1−5 bonds between S beads. The 1−5 Morse bonds account for the formation of an intrachain hydrogen bond along the helical axis while taking into account the steric limits of the polypeptide chain. The 1−3 Morse bonds effectively reduce the angles accessible between adjacent residues, reducing the torsional freedom such that the backbone will properly attain the helical configuration but will not remain fixed while in coil or globular configurations. The equilibrium distance r_e was set to $r_e = 0.9R_c$ for 1−3 Morse bonds (to obtain

dx.doi.org/10.1021/jz301277b | J. Phys. Chem. Lett. 2012, 3, 3081−3087

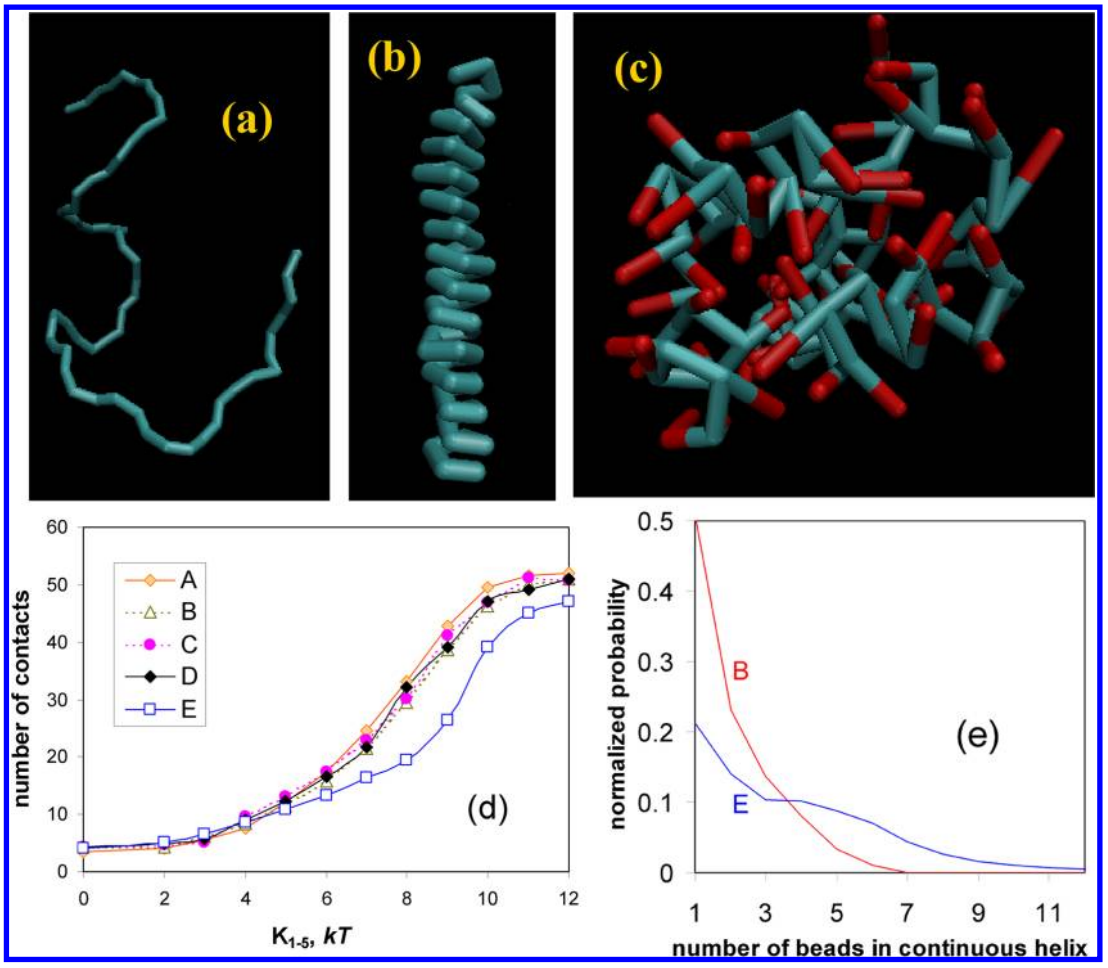

Figure 1. Top: Snapshots of different types configurations obtained in coarse-grained simulations of model peptides; the chain length is 60 model residues; (a) coil-like configuration and (b) α-helical structure, both formed by the A model of the primitive peptide chain composed of skeletal beads; (c) a globular disordered configuration with considerable α-helical content in the E model peptide; hydrophobic beads are shown in red. Bottom: (d) The number of established helix-forming bonds per chain in different model peptides A–E depending on the depth of the Morse potential; (e) the distributions of the lengths of helical fragments for B and E model peptides. The lack of long-range ordering of the polypeptide into helices is consistent with a molten globule containing no persistent secondary structure. Arrows show the conditions, which correspond to the snapshots shown on the top.

the correct angle) and $r_e = 0.6R_c$ for 1–5 Morse bonds, in order to obtain an estimated "vertical step" of the helix. The width of the Morse potentials was set to $\alpha = 8$, and the cutoff was set to $r_M = 2.5R_c$. The potential depth K_{1-3} was set to $12kT$. The Morse potential depth, K_{1-5}, was varied from 0 to $12kT$. The sequence and condition determinants of helix formation are determined by K_{1-5}.

We characterized the tendency for helix formation by the counting the number of helix-forming 1–5 contacts and by determining the distributions of the lengths of continuous helical fragments. Beads separated by four bonds are considered to be in helical contact when the distance between them is below $0.85R_c$, which approximately corresponds to the distance between the carbon and nitrogen of the >C═O···H–N< construction and is slightly less than the α-helix vertical step of 5.4 Å. If such a situation is found, we assume that the chain made the full turn and the helix length is set to zero. If the next S bead also stays in contact with its counterpart, the helix length is increased by 0.25 to make 1 for one full turn and so on. As we continue the forward motion along the chain of S beads, the continuous coil breaks as soon as we find a bead j that is separated from the $j - 4$ bead by a distance exceeding $0.85R_c$. As such, the helix composed of m full turns is characterized by the length equal $m - 1$.

The coil to helix transformation was studied with five characteristic model peptide chains with different compositions of uncharged hydrophobic and hydrophilic beads. Model A is the primitive homopolymer consisting only of S beads without side chains. In model B, hydrophilic side chains modeled as H beads are attached to all skeletal S beads. In model C, one-quarter of the H beads are randomly replaced by hydrophobic T beads; in model D, their share increases to one-half, and in model E, all skeletal S beads have T beads attached. Note that with these model chains, we do not attempt to reproduce real proteins, and as such, model A should not be regarded as a polyglycine chain. Rather, we explore how the model parameters are to be changed to reproduce different characteristic chain conformations.

Figure 1a,b shows the snapshots of typical configurations in model A composed of 60 S beads at two different depths of the Morse potential, $K_{1-5} = 1kT$ and $9kT$. As the helix-forming potential becomes stronger, consistent helical structures emerge from the coil-like configuration. The formation of the helix is countered by increasing hydrophobic interactions that even-

dx.doi.org/10.1021/jz301277b | J. Phys. Chem. Lett. 2012, 3, 3081–3087

tually favor a globular structure, as shown in Figure1c with a snapshot of the most hydrophobic model E at the same strength of the helix-forming potential as model A in Figure 1b that forms an ideal helix.

Quantification of the simulated configurations for the five model peptides is given in Figure 1d,e. The dependence as a function of the Morse potential strength (Figure 1d) illustrates how the number of H-bond-forming contacts increases and a helical structure emerges from a coil as the Morse constant increases. The distribution of helical fragment lengths illustrates the quality of helix formation. Apparently, the transition from coil-like to helical structures is easy to obtain. The question is whether the model is able to qualitatively reproduce the influence of the peptide composition on the tendency to form helixes. For example, an excess of strongly hydrophobic side chains is known to disrupt the helical structures, rather favoring randomly collapsed configurations.[32] It appears that hydrophilic beads have little effect on the system as all model peptides transit into helices at the same Morse potential depth. Only in the most hydrophobic system E do hydrophobic interactions overpower the Morse bonds, and the helical structures are disrupted by strongly hydrophobic side chains, which is quantified by helix fragment length distributions (Figure 1e).

Secondary structures in proteins, like β-strands, β-hairpins, and β-sheets, are caused by possible formation of long-lived and highly correlated hydrogen bonds, which make the chains fold into these specific conformations. In this work, we restrict ourselves to modeling single chains in solutions and focus on the formation of hairpin-like configurations. To study β-structure formation, we introduced torsional rigidity of the S bead skeleton by connecting the beads separated by two bonds by 1−3 harmonic bonds of $1.2R_c$ with $K_b = 160kT/R_c^2$, so that β-strand conformations would correspond to the energy minimum in the absence of all other forces. Beads separated by three or more harmonic bonds were allowed to form Morse bonds with each other with the same width $a = 8$, length $r_e = 0.6R_c$, $R_M = 2.5R_c$, and varying depth K_M.

Figure 2 shows the dependence of the average number of H-bond-forming contacts on the potential depth K_M in a model peptide composed of S beads only. At lower potential depth, interstrand H-bonds contribute negligibly, and a coil conformation prevails. As the depth increases, transitions between coil (Figure 1a) and hairpin configurations (Figure 2b) are confirmed by a bimodal distribution of the average number of contacts (inset in Figure 2a). If the potential depth is increased further, a highly cross-linked globule-type structure is obtained (Figure 2c), which is unphysical. The reason for this is the inability of a model with a spherically symmetric potential to incorporate the direction of hydrogen bonds. Therefore, the chains or their segments may form multiple Morse bonds to any attachment point that happens to be close enough. This unphysical behavior can be avoided by using directional Morse bonds, which is beyond the concise scope of this Letter. The practical range of applicability of the Morse potential in terms of the magnitude of the potential depth lies below the transition to entangled globular conformations shown in Figure 2c. Despite these restrictions, the proposed model seems promising in accounting for β-structure folding and unfolding.

As an instructive example, we consider a model block polypeptide that mimics the main structural features of αSyn. αSyn is a highly conserved 140 residue, 14kD presynaptic protein with a intrinsically disordered monomeric state of unknown function that is expressed in high levels in the brain.[33]

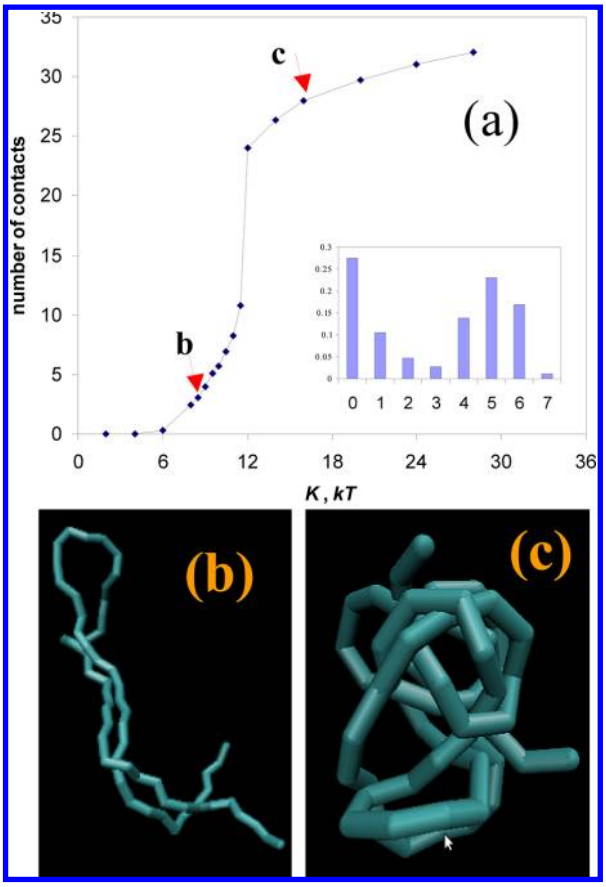

Figure 2. (a) The number of contacts between the Morse bond-forming bead as a function of the Morse force constant. Arrows show the condition to which the snapshots (b,c) are attributed. The inset shows the probability distribution of the number of contacts at $K = 8.5kT$. (b) β-Hairpin configuration. (c) Unphysical globular configuration caused by an excessively strong Morse potential. Arrows show the conditions, which correspond to the snapshots (b) and (c).

Aggregation of αSyn has been implicated in the etiology of PD.[25] Though its conformational ensemble contains little persistent structure, αSyn can attain a partial helical structure when associated with lipid bilayers[34] and interacts with hydrophobic interfaces to activate aggregation into cross-β-containing fibrils.[35] αSyn has three amphipathically distinct domains, reminiscent of a charged-hydrophobic-charged triblock copolymer. Block I represents the N-terminal domain (residues 1−60) that forms α-helices in association with membranes, vesicles, or micelles and is highly charged with a net positive charge at neutral pH; at pH = 7.55, it has 11 positive and 8 negative charges. Block II is the central region (residues 61−95) predominantly consisting of hydrophobic residues, known as the NAC or "non-amyloid β component" because of its initial observation in Alzheimer's disease lesions; it is primarily responsible for aggregation.[36] Block III, the acidic C-terminal region (residues 96−140), contains three highly conserved tyrosine residues[37] and may block aggregation by shielding the NAC from intermolecular interactions.[38] It has 3 positive and 15 negative charges at pH = 7.55, as determined from published pK_a values.[39] Though aggregation of αSyn is implicated in disease states, the protein is stable in solution in the absence of hydrophobic interfaces.[35]

The polypeptide model used the sequence of residues in αSyn, each of which was modeled by the skeleton bead S with

dx.doi.org/10.1021/jz301277b | J. Phys. Chem. Lett. 2012, 3, 3081−3087

one or two T and H beads, as illustrated by the fragment shown in Figure 3. A table with a DPD model of αSyn residues is given

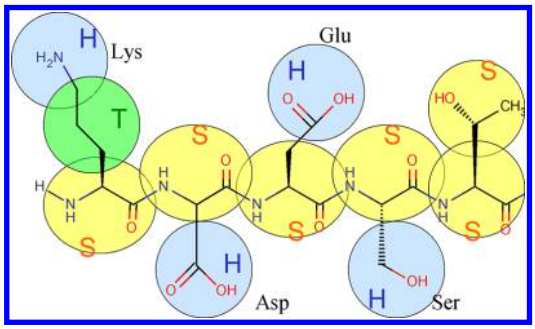

Figure 3. Coarse-grained model of an exemplary peptide section LysAspGluSerThr.

in the Supporting Information. Each skeletal S bead (except for Gly residues) was connected to a side chain, consisting of one or two beads connected by harmonic bonds with no angle rigidity applied (see the Supporting Information). All charged beads were modeled as hydrophilic H beads. Charges were set to the H beads according to the pK_a values for the side chains reported by Nozaki and Tanford.[39] The method of Talaga and Li[19] was employed for the charge assignment at a given solution pH assuming that $Q = \pm 1/(1 + (10^{\pm(pH-pK_a)}))$, where the positive branch accounts for basic residues and the negative branch accounts for acidic residues. These charges, however, are averaged. Fractional charges of residues mean that they are protonated in some peptide molecules and deprotonated in the other. Unable to reproduce protonation/deprotonation reactions in coarse-grained DPD simulations, we assign integer $+e$ and $-e$ charges according to the prevalence of a positive or negative charge at a given pH; the exact table of charges is given in the Supporting Information, Table S2.

The proposed polypetdide model does not represent the whole complexity of αSyn; however, it captured the main differences between the residues in terms of their hyrdophobicity/hydrophylicity and charges. The model clearly distinguished between the three blocks in αSyn, reproducing the actual sequence of residues. Secondary structure formation in block I was mimicked with 1−5 Morse potentials with $K_{1-5} = 9\ kT$ as in model A, which produced a well-defined α-helix without the side chains and charges, Figure 1b. That is, we applied different Morse bond schemes for block I and blocks II and III. For the chemical composition of αSyn, block 1 displayed a disordered structure with substantial α-helical content. Blocks II and III were treated using the model used for modeling β-structures with the Morse potential of $K_M = 8.5kT$, which corresponds to coil configuration with some β content for the skeletal peptide of S beads without side chains (Figure 2), which may turn to a globule configuration if the chain is long enough.

We considered the behavior of the model αSyn polypeptide at two different acidities, pH = 7 and 4. Characteristic snapshots given in Figure 4 show the effects of solvent acidity on the polypeptide conformations. To focus on the secondary structures, we present only skeletal beads shown in green in block I, red in block II, and blue in block III. The hydrophobic interactions make block II collapse into a globule at both pHs considered. Block III experiences a transition from a coil to a globular configuration with a change of pH from 7 to 4 as entropy and electrostatic forces caused by the protonation of

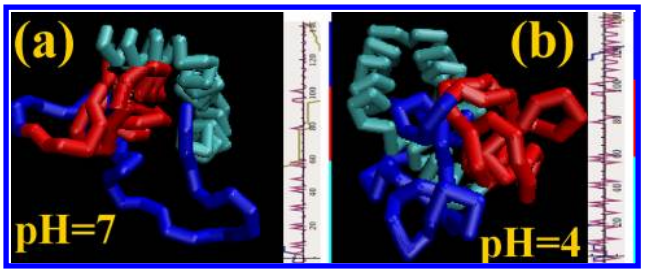

Figure 4. Characteristic snapshots of DPD simulations of αSyn polypeptide model at pH = 7 (a) and 4 (b). The colors show three blocks of the protein, green - block I, red - block II, and blue - block III (only skeletal particles are shown). The insets show charge distributions along the molecule. Block I (60 amino acids) has a substantial α-helix content and is positively charged at pH = 4. Block II (35 amino acids) has low charge and primarily consists of hydrophobic residues. Block III (45 amino acids) bears a strong negative charge at pH = 7, which makes it adopt a random coil configuration with some β-strand content, and it is mostly hydrophobic and collapsed at pH = 4 when acidic residues associate.

acidic Glu and Arg residues are overpowered by the hydrophobic attraction of more "massive" amino acids. Overall, the radius of gyration of the polypeptide changes from 26.1 Å at acidic conditions to 27.8 Å at neutral conditions, and the radius of gyration of block III increases from 13.5 to 18.5 Å. A relatively small variation of the overall size of the polypeptide compared with the increase of block III is explained by the fact that block III tends to align with the positively charged block I. This example shows the capabilities of the proposed DPD model of proteins in modeling complex polypeptide structures.

In summary, we suggest an original approach to accounting for H-bond formation within the general DPD framework that may make the DPD method a competitive alternative to CGMD for modeling equilibrium and dynamic properties of proteins and polypeptides, especially during their transport in a confined environment. DPD due to its soft potentials allows for long integration steps and convenient introduction of random and drag forces that are necessary for accurate description of hydrodynamics. The suggested approach suffices to qualitatively describe transitions between coiled, globular, and α- and β- structures in model peptides. Our simulations showed a qualitatively correct influence of the hydrophobicity of side chains on the transitions between α-helical and disordered structures of model peptides, as well as the influence of electrostatic forces on the conformations of peptide chains. The pattern of fractional secondary structure content was consistent with a cooperative transition. At the same time, it should be noted that a quantitative description of polypeptide secondary structures requires significant refinement of the proposed approach. A careful evaluation of repulsion parameters needs to be performed based on well-defined thermodynamic properties, such as activity coefficients of reference solutions. The lengths and rigidities of the harmonic bonds between skeletal and side-chain groups can be evaluated from atomistic MD results for solutions of amino acids and different peptides because atomistic force field parameters for this group of compounds are established in the literature with sufficient accuracy.[40] The parameters of the Morse bonds between skeletal beads should be evaluated from the qualitative and quantitative data on secondary structures of simple (first of all homogeneous) polypeptides. With the further force field development, the proposed approach promises to allow for modeling of the

dx.doi.org/10.1021/jz301277b | J. Phys. Chem. Lett. 2012, 3, 3081−3087

condition and sequence effects on polypeptide structure while maintaining the feasibility of long time/length calculations with correct hydrodynamics.

■ ASSOCIATED CONTENT

Supporting Information

Tables of parameters of the model, table of the charges of residue side chains used in DPD simulations, calibration curves for assigning like parameters of conservative repulsion between identical beads, and description of simulation details. This material is available free of charge via the Internet at http://pubs.acs.org.

■ AUTHOR INFORMATION

Corresponding Author

*E-mail: aneimark@rutgers.edu.

Notes

The authors declare no competing financial interest.

■ ACKNOWLEDGMENTS

The authors thank Shuang Yang (ICCAS P.R.C.) for calibration curves shown in Figure S1. This work is supported in part by the NSF grant 1064170 (A.V.N.), NSF NIRT 0609000, and NIH R01GM071684 (D.S.T.). The content is solely the responsibility of the authors and does not necessarily represent the official views of the National Institute of General Medical Sciences or the National Institutes of Health.

■ REFERENCES

(1) Gautieri, A.; Russo, A.; Vesentini, S.; Redaelli, A.; Buehler, M. J. Coarse-Grained Model of Collagen Molecules Using an Extended Martini Force Field. *J. Chem. Theory Comput.* **2010**, *6*, 1210−1218.

(2) Korolev, N.; Lyubartsev, A. P.; Nordenskiold, L. Computer Modeling Demonstrates That Electrostatic Attraction of Nucleosomal DNA Is Mediated by Histone Tails. *Biophys. J.* **2006**, *90*, 4305−4316.

(3) Lopez, C. A.; Rzepiela, A. J.; De Vries, A. H.; Dijkhuizen, L.; Huenenberger, P. H.; Marrink, S. J. Martini Coarse-Grained Force Field: Extension to Carbohydrates. *J. Chem. Theory Comput.* **2009**, *5*, 3195−3210.

(4) Marchut, A. J.; Hall, C. K. Side-Chain Interactions Determine Amyloid Formation by Model Polyglutamine Peptides in Molecular Dynamics Simulations. *Biophys. J.* **2006**, *90*, 4574−4584.

(5) Marchut, A. J.; Hall, C. K. Effects of Chain Length on the Aggregation of Model Polyglutamine Peptides: Molecular Dynamics Simulations. *Proteins: Struct., Funct., Bioinf.* **2007**, *66*, 96−109.

(6) Monticelli, L.; Kandasamy, S. K.; Periole, X.; Larson, R. G.; Tieleman, D. P.; Marrink, S.-J. The Martini Coarse-Grained Force Field: Extension to Proteins. *J. Chem. Theory Comput.* **2008**, *4*, 819−834.

(7) Morozova, D.; Guigas, G.; Weiss, M. Dynamic Structure Formation of Peripheral Membrane Proteins. *Plos Comput. Biol.* **2011**, 7.

(8) Nguyen, H. D.; Hall, C. K. Spontaneous Fibril Formation by Polyalanines; Discontinuous Molecular Dynamics Simulations. *J. Am. Chem. Soc.* **2006**, *128*, 1890−1901.

(9) Wang, Y. L.; Laaksonen, A.; Lu, Z. Y. Specific Binding Structures of Dendrimers on Lipid Bilayer Membranes. *Phys. Chem. Chem. Phys.* **2012**, *14*, 8348−8359.

(10) Wang, Y. T.; Voth, G. A. Molecular Dynamics Simulations of Polyglutamine Aggregation Using Solvent-Free Multiscale Coarse-Grained Models. *J. Phys. Chem. B* **2010**, *114*, 8735−8743.

(11) Matysiak, S.; Debenedetti, P. G.; Rossky, P. J. Role of Hydrophobic Hydration in Protein Stability: A 3d Water-Explicit Protein Model Exhibiting Cold and Heat Denaturation. *J. Phys. Chem. B* **2012**, *116*, 8095−8104.

(12) Venturoli, M.; M.M., S.; Kranenburg, M.; Smit, B. Mesoscopic Models of Biological Membranes. *Phys. Rep.* **2006**, *437*, 1−54.

(13) Seo, M.; Rauscher, S.; Pomes, R.; Tieleman, D. P. Improving Internal Peptide Dynamics in the Coarse-Grained Martini Model: Toward Large-Scale Simulations of Amyloid- and Elastin-Like Peptides. *J. Chem. Theory Comput.* **2012**, *8*, 1774−1785.

(14) Smith, A. V.; Hall, C. K. Protein Refolding Versus Aggregation: Computer Simulations on an Intermediate-Resolution Protein Model. *J. Mol. Biol.* **2001**, *312*, 187−202.

(15) Branden, C.; Tooze, J. *Introduction to Protein Structure*, 2nd ed.; Garland Publishing: New York, 1999.

(16) Digambaranath, J. L.; Campbell, T. V.; A., C.; Mcphail, M. J.; Stevenson, K. E.; Zohdy, M. A.; Finke, J. M. An Accurate Model of Polyglutamine. *Proteins: Struct., Funct. Bioinf.* **2011**, *79*, 1427.

(17) De Meyer, F. J. M.; Rodgers, J. M.; Willems, T. F.; Smit, B. Molecular Simulation of the Effect of Cholesterol on Lipid-Mediated Protein−Protein Interactions. *Biophys. J.* **2010**, *99*, 3629−3638.

(18) Schneller, W.; Weaver, D. L. Simulation of α-Helix Coil Transitions in Simplified Polyvaline — Equilibrium Properties and Brownian Dynamics. *Biopolymers* **1993**, *33*, 1519−1535.

(19) Talaga, D. S.; Li, J. Single-Molecule Protein Unfolding in Solid State Nanopores. *J. Am. Chem. Soc.* **2009**, *131*, 9287−9297.

(20) Espanol, P.; Warren, P. Statistical-Mechanics of Dissipative Particle Dynamics. *Europhys. Lett.* **1995**, *30*, 191−196.

(21) Groot, R. D.; Rabone, K. L. Mesoscopic Simulation of Cell Membrane Damage, Morphology Change and Rupture by Nonionic Surfactants. *Biophys. J.* **2001**, *81*, 725−736.

(22) Dutt, M.; Kuksenok, O.; Nayhouse, M. J.; Little, S. R.; Balazs, A. C. Modeling the Self-Assembly of Lipids and Nanotubes in Solution: Forming Vesicles and Bicelles with Transmembrane Nanotube Channels. *ACS Nano* **2011**, *5*, 4769−4782.

(23) Guigas, G.;Morozova, D.;Weiss, M., Exploring Membrane and Protein Dynamics with Dissipative Particle Dynamics In *Advances in Protein Chemistry and Structural Biology, Vol 85: Computational Chemistry Methods in Structural Biology*; Christov, C., Ed.; Elsevier Academic Press Inc.: San Diego, CA, 2011; pp 143−182.

(24) Venturoli, M.; Smit, B.; Sperotto, M. M. Simulation Studies of Protein-Induced Bilayer Deformations, and Lipid-Induced Protein Tilting, on a Mesoscopic Model for Lipid Bilayers with Embedded Proteins. *Biophys. J.* **2005**, *88*, 1778−1798.

(25) Spillantini, M. G.; Crowther, R. A.; Jakes, R.; Cairns, N. J.; Lantos, P. L.; Goedert, M. Filamentous α-Synuclein Inclusions Link Multiple System Atrophy with Parkinson's Disease and Dementia with Lewy Bodies. *Neurosci. Lett.* **1998**, *251*, 205−208.

(26) Perkins, S. J. Protein Volumes and Hydration Effects. *Eur. J. Biochem.* **1986**, *157*, 169−180.

(27) Morse, P. M. Diatomic Molecules According to the Wave Mechanics. II. Vibrational Levels. *Phys. Rev.* **1929**, *34*, 57−64.

(28) Rappe, A. K.; Casewit, C. J.; Colwell, K. S.; Goddard, W. A.; W.M., S. UFF, A Full Periodic Table Force Field for Molecular Mechanics and Molecular Dynamics Simulations. *J. Am. Chem. Soc.* **1992**, *114*, 10024−10039.

(29) Toukan, K.; Rahman, A. Molecular-Dynamics Study of Atomic Motions in Water. *Phys. Rev. B* **1985**, 2643−2648.

(30) Muller, E. A.; Rull, L. F.; Vega, L. F.; Gubbins, K. E. Adsorption of Water on Activated Carbons: A Molecular Simulation Study. *J. Phys. Chem.* **1996**, *100*, 1189−1196.

(31) Schiffer, M.; Edmundson, A. B. Use of Helical Wheels to Represent the Structures of Proteins and to Identify Segments with Helical Potential. *Biophys. J.* **1967**, *7*, 121−135.

(32) Scholtz, J. M.; Baldwin, R. L. The Mechanism of α-Helix Formation by Peptides. *Annu. Rev. Biophys. Biomol. Struct.* **1992**, *21*, 95−118.

(33) Rochet, J. C.; Lansbury, P. T. Amyloid Fibrillogenesis: Themes and Variations. *Curr. Opinion Struct. Biol.* **2000**, *10*, 60−68.

(34) Shvadchak, V. V.; Yushchenko, D. A.; Pievo, R.; Jovin, T. M. The Mode of α-Synuclein Binding to Membranes Depends on Lipid Composition and Lipid to Protein Ratio. *FEBS Lett.* **2011**, *585*, 3513−3519.

(35) Pronchik, J.; He, X.; Giurleo, J. T.; Talaga, D. S. In Vitro Formation of Amyloid from α-Synuclein Is Dominated by Reactions at Hydrophobic Interfaces. *J. Am. Chem. Soc.* **2010**, *132*, 9797−9803.
(36) El-Agnaf, O. M. A.; Bodles, A. M.; Guthrie, D. J. S.; Harriott, P.; Irvine, G. B. The N-Terminal Region of Non-a Beta Component of Alzheimer's Disease Amyloid Is Responsible for Its Tendency to Assume Beta-Sheet and Aggregate to Form Fibrils. *Eur. J. Biochem.* **1998**, *258*, 157−163.
(37) Kim, T. D.; Paik, S. R.; Yang, C. H. Structural and Functional Implications of C-Terminal Regions of α-Synuclein. *Biochemistry* **2002**, *41*, 13782−13790.
(38) Uversky, V. N. Neuropathology, Biochemistry, and Biophysics of α-Synuclein Aggregation. *J. Neurochem.* **2007**, *103*, 17−37.
(39) Nozaki, Y.; Tanford, C. Examination of Titration Behavior. *Methods Enzymol* **1967**, *11*, 715−734.
(40) Meli, M.; Colombo, G. Molecular Simulations of Peptides: A Useful Tool for the Development of New Drugs and for the Study of Molecular Recognition. *Methods Mol. Biol.* **2009**, *570*, 77−153.